ACS Catalysis

Letter

pubs.acs.org/acscatalysis

Origin of Catalytic Effect in the Reduction of CO_2 at Nanostructured TiO_2 Films

Ganganahalli K. Ramesha,[†] Joan F. Brennecke,*[,‡] and Prashant V. Kamat*[,†,‡,§]

[†]Radiation Laboratory, [‡]Department of Chemical and Biomolecular Engineering, [§]Department of Chemistry and Biochemistry, University of Notre Dame, South Bend, Indiana 46556, United States

Supporting Information

ABSTRACT: Electrocatalytic activity of nanostructured TiO_2 films toward the reduction of CO_2 is probed by depositing a nanostructured film on a glassy carbon electrode. The one-electron reduction of CO_2 in acetonitrile seen at an onset potential of −0.95 V (vs NHE) is significantly lower than the one observed with a glassy carbon electrode. The electrocatalytic role of TiO_2 is elucidated through spectroelectrochemistry and product analysis. Ti^{3+} species formed when the TiO_2 film is subjected to negative potentials have been identified as active reduction sites. Binding of CO_2 to catalytically active Ti^{3+} followed by the electron transfer facilitates the initial one-electron reduction process. Methanol was the primary product when the reduction was carried out in wet acetonitrile.

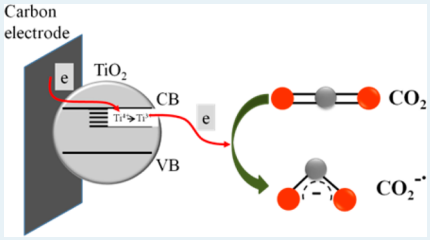

KEYWORDS: *CO_2 reduction, TiO_2, electrocatalysis, electrochemical reduction, Faradaic efficiency, spectroelectrochemistry, methanol, Ti^{3+} states, C_1 fuel formation*

Investigations which are designed to find new and feasible approaches to carbon dioxide reduction have gained momentum in recent years. Homogeneous catalysis, electrocatalysis, and semiconductor-assisted photocatalysis are projected to be viable techniques.[1−7] The reduction of CO_2 to produce hydrocarbons or alcohols involves proton-coupled multielectron processes.[8] As has been discussed in recent studies, even a single proton-coupled electron transfer event is complex and requires a well-thought-out design of catalysts.[9] In this context, TiO_2 has been shown to induce proton-coupled electron transfer to CO_2 under bandgap excitation. However, spectroscopic evidence to date, which can conclusively prove multiple electron transfer at semiconductor nanoparticles is lacking. Even in cases where two-electron reduction is thermodynamically favored over a single electron transfer, the spectroscopic measurements suggest sequential one-electron reduction steps.[10,11] The major hurdle in CO_2 reduction is the barrier imposed by the first step of one-electron reduction. Thermodynamics requires a potential more negative than −1.9 V versus NHE (ΔG^0 = +183.32 kJ mol^{-1}) to induce the one-electron reduction of CO_2 to $CO_2^{-\bullet}$ radical.[9,12] However, electrocatalysts and homogeneous catalysts have been shown to promote CO_2 reduction at relatively lower potentials. Electrocatalytically active electrode materials, such as Au,[13] Cu,[14] Pt/TiO_2,[15] Ir−Pd alloy,[16] and metal complexes,[17,18] exhibit remarkable selectivity toward the formation of reduction products ranging from CO to CH_4.

In recent years, TiO_2 has been identified as a potential photocatalyst to reduce CO_2.[19] Reduction products, such as aldehydes, carboxylic acids, alcohols, and hydrocarbons, have been identified.[20−26] It is important to note the thermodynamic limitations of TiO_2 as the reductant. Its conduction band is energetically less reductive (−0.5 V vs NHE at pH 7) than what is required for the one-electron reduction of CO_2. This energetics favors reduction of molecules such as O_2, methyl viologen, or metal ions, following bandgap excitation of TiO_2.[27,28] Infrared spectroscopic and electron paramagnetic resonance (EPR) studies have indicated that catalytically active (Ti^{3+}-O^-) sites formed at the TiO_2 surface are responsible for CO_2 reduction.[29−31] The role of surface acid−base sites, as well as polymorphs, in surface interaction with CO_2 has been investigated by Fourier transform infrared (FTIR) techniques.[25,32] Recent theoretical studies of CO_2 reduction on TiO_2 surfaces show that it is defect sites and/or reduced surface states of TiO_2 that result in favorable charge transfer from TiO_2 to CO_2.[33,34] At the outset, such a photocatalytic approach seems attractive, yet, many fundamental questions remain unanswered. For example, TiO_2 is a strong oxidant which can mineralize hydrocarbons and other organics into CO_2 at the interface when subjected to UV irradiation. The photogenerated hole and hydroxyl radical oxidation at the TiO_2 interface has been extensively studied for various organics, such as formic acid and alcohols.[35−37] In this context, questions have been raised whether products identified in the TiO_2 assisted CO_2 reduction are the result of oxidation of organic impurities rather than the reduction of CO_2.[19,26]

The arguments made above raise two simple questions: What are the thermodynamic requirements for achieving CO_2 reduction at a TiO_2 electrode? If so, what are the active sites that are responsible for electrocatalytic activity? In order to seek

Received: February 27, 2014
Revised: August 12, 2014
Published: August 18, 2014

   dx.doi.org/10.1021/cs500730w | ACS Catal. 2014, 4, 3249−3254

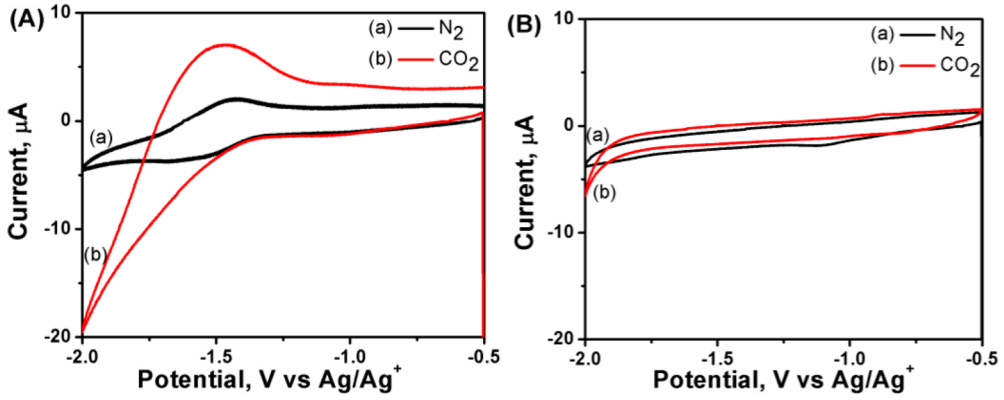

Figure 1. Cyclic voltammograms of (A) TiO_2 modified GCE and (B) bare GCE in 0.1 M TEAP/acetonitrile. Curves (a) and (b) correspond to the electrolyte saturated with N_2 and CO_2, respectively. Scan rate: 0.05 V/s.

answers to these questions, we have conducted electrochemical reduction of CO_2 using nanostructured TiO_2 films. The results of electrochemical measurements that illustrate the electrocatalytic role of TiO_2 are discussed.

ELECTROCATALYTIC ROLE OF TIO_2

In photocatalysis, a semiconductor nanoparticle or nanostructured semiconductor film is subjected to bandgap excitation. The photogenerated holes and electrons participate in the oxidation and reduction processes at the semiconductor/electrolyte interface. By suitably scavenging one of the charge carriers (e.g., scavenging of electrons by O_2 or scavenging of holes by methanol), one can enhance the selectivity of the reduction or oxidation process. On the other hand, electrochemical measurements provide a convenient way to directly probe the reduction process. Use of nonaqueous solvents, such as acetonitrile, provide a wider electrochemical window to carry out reductions (up to −2.5 V vs Ag/Ag^+ reference) and exclude protonation equilibria that one encounters in aqueous media (e.g., $H_2CO_3 \Leftrightarrow HCO_3^- \Leftrightarrow CO_3^{2-}$).

In the present study, we deposited a thin film of TiO_2 on a glassy carbon electrode (GCE) by treating the electrode surface with titanium isopropoxide. (It should be noted that the TiO_2 electrode is conductive in the cathodic scan and hence can be used to monitor the reduction process.) The working electrode (GCE, or GCE/TiO_2) was introduced in a three arm electrochemical cell containing 0.1 M tetraethylammonium perchlorate (TEAP) in acetonitrile with Ag/Ag^+ as the reference electrode and Pt as the counter electrode. Figure 1 shows the cyclic voltammograms of GCE with and without TiO_2 modification in N_2- and CO_2-saturated electrolyte. In a N_2 atmosphere, the GCE/TiO_2 electrode shows a reduction peak at −1.5 V (Figure 1A), corresponding to the reduction of Ti^{4+} sites in TiO_2 to form Ti^{3+}. The Ti^{3+} species can be stabilized if smaller cations, such as H^+ or Li^+, are available in the electrolyte. Details on the electrochemistry of TiO_2 films and formation of Ti^{3+} species in TiO_2 films under controlled electrochemical potentials have been discussed previously.[38]

When the cyclic voltammogram was recorded in a CO_2-saturated electrolyte, we observe an increase in the cathodic current, providing evidence for the reduction of CO_2. However, the onset of this reduction is indistinguishable from that of Ti^{4+} reduction. Similar indistinguishable photocurrent at the TiO_2 electrode has been seen when an electrochemical bias was applied in the presence of pyridinium cations.[15] The magnitude of the current increase seen at potentials more negative than −1.5 V versus Ag/Ag^+ in scan (b) is significantly greater than that in scan (a) of Figure 1A, thus confirming the ability of TiO_2 to reduce CO_2.

It is interesting to note that there is no evidence for CO_2 reduction at potentials in the same scan range in the absence of TiO_2 (Figure 1B). Blank experiments carried out with GCE alone do not show any current arising from CO_2 reduction under the linear sweep with potentials extending up to −2.0 V versus Ag/Ag^+ reference. These results confirm that the TiO_2 surface acts as an electrocatalyst, by lowering the potential required for the reduction of CO_2. On the basis of first-principles calculations, Zapol and co-workers predicted a decrease in the reduction potential of adsorbed CO_2 on a (101) surface of TiO_2 by 0.24 V as compared to the reduction potential of a CO_2 molecule in aqueous solution.[33] This lowering of reduction potential can be attributed to the monodentate and bidentate configuration of CO_2 with TiO_2, which in turn facilitates charge transfer through hybridized orbitals (Scheme 1). Details on the influence of the strength of Lewis acidity and oxygen deficiency on the binding of CO_2 can be found elsewhere.[33]

Scheme 1. Adsorption of CO_2 to a TiO_2 Surface: (a) Bidentate and (b) Monodentate Interactions Which Are Dictated by the Lewis Acidity of the Surface. (c) Adsorption of CO_2 at the Oxygen Vacancy (or Ti^{3+}) Site. Adapted from Ref 32. Copyright 2013, American Chemical Society

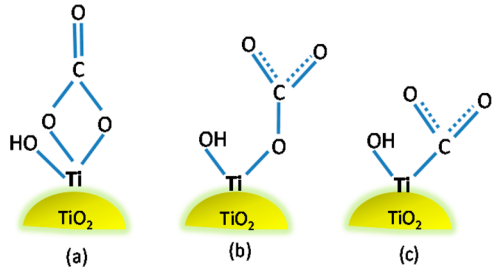

We also wanted to establish the reversibility and reproducibility of the TiO_2-assisted electrocatalytic CO_2 reduction. We switched the purging gas (N_2 and CO_2) alternatively in the electrochemical cell while monitoring the current at fixed potentials of −1.3 V and −1.8 V versus Ag/Ag^+ reference (Figure 2). When the GCE/TiO_2 electrode was maintained at −1.3 V, we do not see any change in the current in response to purging of N_2 or CO_2 gas. However, at a potential of −1.8 V,

dx.doi.org/10.1021/cs500730w | ACS Catal. 2014, 4, 3249−3254

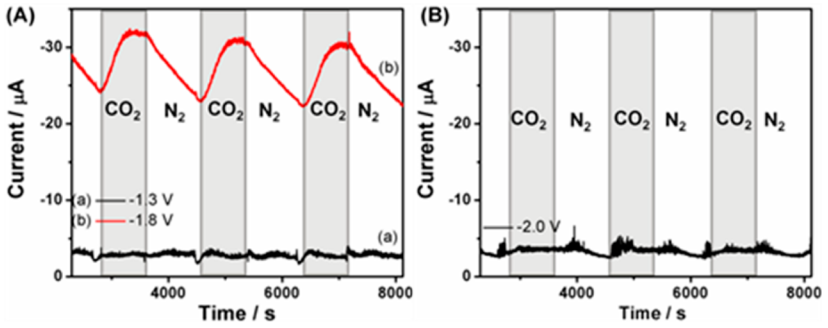

Figure 2. Current−time profiles for (A) TiO_2-modified GCE maintained at (a) −1.3 and (b) −1.8 V; and (B) unmodified GCE at −2.0 V. Shaded and blank regions correspond to switching between CO_2 and N_2 purging gas, respectively. The electrolyte was 0.1 M TEAP in ACN, and the reference electrode was Ag/Ag^+.

we see an increase in the current from 24 μA to about 32 μA when the purging gas was switched from N_2 to CO_2. The reduction of CO_2 can thus be observed only at potentials more negative than −1.3 V versus Ag/Ag^+ reference electrode.

As the solution becomes saturated with CO_2, we observe a steady current emerging from the CO_2 reduction. When the purge gas was switched to N_2, we see a decrease in the current as CO_2 in the solution is depleted. The effect of purge gas on the current monitored over several switching cycles demonstrates the reversibility and reproducibility of the CO_2 reduction by the TiO_2 film deposited on a GCE. We also repeated this experiment with an unmodified GCE under switching cycles of N_2 and CO_2 purge gas. No change in the reduction current was seen even when the GCE was held at a potential of −2 V (Figure 2B).

The reduction seen in Figure 1A and 2A arises from one-electron reduction of CO_2 to form $CO_2^{-\bullet}$. Although multielectron coupled with proton transfer has been invoked in photocatalytic reduction of CO_2,[19,31] we could not gather any evidence for multielectron transfer in our electrochemical experiments. If we were to see multiple electron reduction, we would have seen the reduction at much lower potentials (E = −0.53 — −0.61 V vs NHE for $2e/2H^+$ reductions). As evidenced in the present experiments, we observe only one-electron reduction at −0.95 V vs NHE as the initial or first step in the overall reduction of CO_2 to produce C_1 products. Subsequent reductions at this applied potential are favored to produce multielectron reduction products.

These experiments confirm that the CO_2 reduction proceeds with one-electron reduction as the primary step. It is important to note that this one-electron reduction thermodynamically limits the overall reduction of CO_2. Once the one-electron reduction is achieved, subsequent reductions proceeds with ease as they demand relatively low energy.

■ ROLE OF Ti^{3+} IN THE REDUCTION OF CO_2

As shown earlier, the reduction potential for CO_2 in aprotic solvents using a mercury electrode (no TiO_2) is −1.9 V versus NHE.[39] The decrease in electrochemical reduction potential for CO_2 with TiO_2 (−1.5 V vs Ag/Ag^+ or −0.95 V vs NHE) illustrates the catalytic role of a TiO_2 film deposited on the GCE. Because the observed onset potential of CO_2 reduction coincides with the reduction of Ti^{4+} (Figure 1A), one expects that the Ti^{3+} formed at the oxygen vacancy sites will facilitate CO_2 reduction.

$$(TiO_2)Ti^{4+} + e \rightarrow (TiO_2)Ti^{3+}$$

$$(TiO_2)Ti^{3+} + CO_2 \rightarrow (TiO_2)Ti^{4+} + CO_2^{-\cdot} \quad (2)$$

Earlier spectroscopic studies have indicated binding of CO_2 to the TiO_2 surface through monodentate and bidentate configurations.[26,32] In particular, binding of CO_2 to the oxygen-deficient Ti^{3+} is of interest in achieving charge transfer. Thus, it becomes apparent that the Ti^{3+} sites are the catalytically active sites promoting the reduction of CO_2 (Scheme 2).

Scheme 2. Electrochemical Conversion of Ti^{4+} to Ti^{3+} and Electron Transfer from Ti^{3+} to CO_2 Resulting in $CO_2^{-\bullet}$

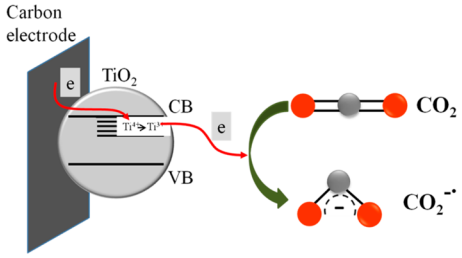

In order to further ascertain the role of Ti^{3+} in the CO_2 reduction, we carried out TiO_2 reduction first in N_2 atmosphere using $LiClO_4$ as supporting electrolyte. Previously, it has been shown that small cations, such as Li^+, associate within the TiO_2 network when Ti^{4+} sites are reduced to Ti^{3+}, and facilitate its stabilization.[38] When a GCE/TiO_2 electrode is subjected to −1.8 V in N_2-saturated acetonitrile containing $LiClO_4$, the Ti^{3+} species formed in these films remain stabilized as Li^+ ions and compensate the charge in the lattice. We then transferred this electrode in a CO_2 reduction experiment (analogous to the experiment in Figure 1A). The Li^+-stabilized TiO_2 electrodes failed to show increased current response corresponding to CO_2 reduction in the cyclic voltammogram (Figure S1 in Supporting Information (SI)). Association of Li^+ with Ti^{3+} would mean that the Ti^{3+} sites are no longer available for interacting with CO_2. By contrast, when the CO_2 reduction with TiO_2 is carried out in TEAP solutions, the Ti^{3+} sites remain active because the bulkier tetraethylammonium cations fail to block the active sites. These active sites catalyze one electron reduction of TiO_2.

In another set of experiments, we employed spectroelectrochemistry to monitor the formation of Ti^{3+} within the TiO_2. The spectroelectrochemical cell consisted of a transparent electrode coated with a TiO_2 film placed in the sample compartment of a UV−vis spectrophotometer. The absorption spectra were recorded as a function of time, while applying a

dx.doi.org/10.1021/cs500730w | ACS Catal. 2014, 4, 3249−3254

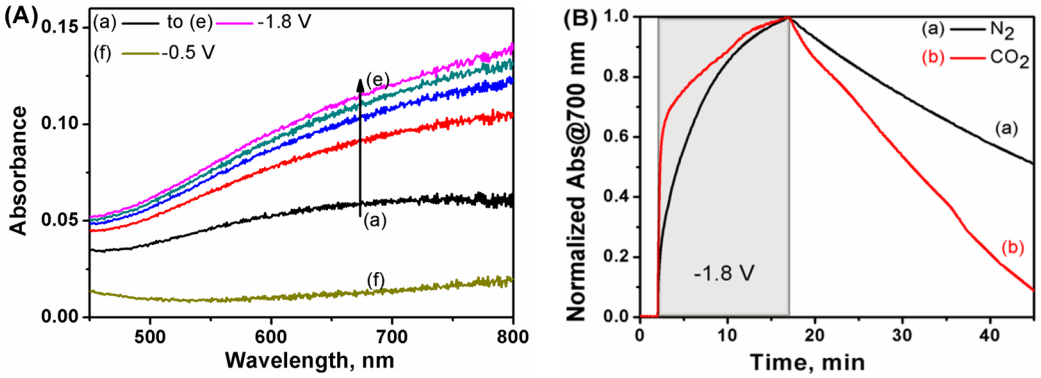

Figure 3. (A) Absorption spectra of a TiO_2-modified conducting glass (FTO) electrode in contact with N_2-purged acetonitrile containing 0.1 M TEAP recorded in a spectroelectrochemical set up. The spectra (a) to (e) were recorded after 3, 6, 9, 12, and 15 min following the application of potential of −1.8 V vs Ag/Ag^+ reference. The spectrum (f) was recorded after reversing the potential to −0.5 V. (B) Plot of normalized absorbance vs time at 700 nm in 0.1 M TEAP/AcN saturated with (a) N_2 and (b) CO_2 (shaded region represents time where constant potential of −1.8 V is maintained at the working electrode).

potential of −1.8 V (spectra a−e in Figure 3A). The absorbance in the red and infrared region increases with time when the applied potential was maintained at −1.8 V versus Ag/Ag^+. These absorbance characteristics are similar to those obtained from UV irradiation of TiO_2 colloids in ethanol and confirm the formation of Ti^{3+}.[38] The absorbance becomes steady after a few minutes following the application of constant potential. Upon reversing the potential from −1.8 V to −0.5 V (curve (f) of Figure 3A), the absorbance in the red-infrared region disappears, consistent with regeneration of Ti^{4+}. These absorption changes confirm the reversibility of Ti^{3+} formation and its stability under an applied potential of −1.8 V.

In order to follow the reactivity of CO_2 toward Ti^{3+}, we repeated in situ spectroelectrochemical experiments by monitoring the absorbance change at 700 nm following the application of the potential of −1.8 V versus Ag/Ag^+ for 15 min (shaded region, Figure 3B). The absorption at 700 nm (corresponding to the formation of Ti^{3+}) increased with time and leveled off somewhat after 15 min. The 15 min absorbance was higher in CO_2-saturated solution than in N_2-saturated solution (note that Figure 3B is normalized with the maximum absorbance in each case). When the applied potential was turned off after 15 min (by disconnecting the electrode from the electrochemical circuit), the absorption at 700 nm slowly decayed. The decay occurred at a faster rate when CO_2 was present in the spectroelectrochemical cell, thus confirming its ability to scavenge the charge from Ti^{3+} (reaction 2). On the basis of these spectroelectrochemical measurements, we can conclude that the CO_2 bound to the TiO_2 surface is responsible for increased disappearance rate of Ti^{3+}. The regeneration of Ti^{4+} is expected to involve electron transfer between Ti^{3+} and CO_2 to produce $CO_2^{-\bullet}$, thus prompting the primary step in the electrocatalytic reduction process.

FATE OF REDUCED CO_2

Once the uphill reaction of one-electron reduction is achieved, successive reductions are thermodynamically favorable, as they occur at potentials lower than the one required for the formation of $CO_2^{-\bullet}$.[12] The reduction of CO_2 to $CO_2^{-\bullet}$ is an irreversible process because $CO_2^{-\bullet}$undergoes subsequent transformations. The $CO_2^{-\bullet}$ can either dimerize to form oxalate anion or undergo successive reduction to produce C_1 products such as CO. If there is a proton source available in the medium, other C_1 products such as formaldehyde, methanol methane are also formed.[31] The reaction pathway with which one observes a specific product accumulation depends upon the nature of the electrode employed and the polarity/functionality of the medium. For example, gold electrodes have been shown to facilitate CO formation, whereas copper electrodes are known to promote formation of methane.[40] Similarly, coexisting electrolyte species such as ionic liquid, [emim]-[Tf2N] can also dictate the course of reduction pathway and hence the accumulation of products.[41,42]

Product analysis following the electrolysis indicated methanol as the major product during the electrolysis at TiO_2 electrode. The methanol concentration was determined by monitoring the peak area in GC-MS corresponding to m/z value of 31 (CH_2OH^+). Typical methanol concentrations observed during reduction of CO_2 in wet acetonitrile were in the range of 2−3 mM during 1 h of electrolysis (Figure S4 in the SI). In another experiment, we also determined the Faradaic efficiency by determining the charge flowed through the circuit (Figure 4). A representative trace showing the charge−time profile recorded during electrolysis is shown in the SI (Figure S2). Nearly 90% efficiency achieved in these experiments demonstrates the effectiveness of the electrocatalytic process.

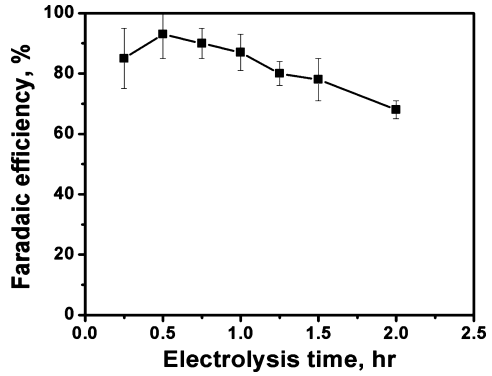

Figure 4. Dependence of Faradaic efficiency on the electrolysis time. The Faradaic efficiency was measured from the amount of methanol formed during electrolysis and amount of charge flowed through the circuit. TiO_2-modified carbon (Toray paper) electrode was maintained at an applied potential of −2.0 V in CO_2 saturated 0.1 M TEAP/acetonitrile (water content: 0.33 M).

dx.doi.org/10.1021/cs500730w | ACS Catal. 2014, 4, 3249−3254

The blank experiment carried out without TiO_2 (i.e., only with Toray paper electrode) under the same experimental conditions did not produce any detectable amounts of methanol. The decrease in the Faradaic efficiency with increased electrolysis time was attributed to the crossover of methanol product to the counter electrode. (See Figure S3 in the Supporting Information for control experiments. The decrease in methanol concentration confirms the permeability of the Nafion membrane, which was used to separate the two electrode compartments.)

Earlier photocatalytic studies carried out with TiO_2 in aqueous medium have shown selectivity toward methanol formation.[43] The adventitious water present in the acetonitrile plays a key role in providing the proton source. We confirmed the role of water by increasing the water content in acetonitrile. Indeed, greater concentration of water increased the amount of methanol produced (Figure S4). The TiO_2 surface is sensitive to protonation and its surface is dominated by Ti−OH groups at neutral pH. As shown previously, the binding of Ti^{3+} to CO_2 leaves the reduced form in close vicinity to −OH groups.[27] Further reduction of $CO_2^{-\bullet}$ in a protic environment is expected to generate methanol. Other reductive species such as H, methoxyl, $\bullet OCH_3$, and methyl, $\bullet CH_3$, radicals formed as reaction intermediates are likely to contribute to the formation of methanol. The formation of such intermediates in the presence of water has been confirmed through EPR measurements.[31] The relatively high Faradaic efficiency observed in the present electrochemical reduction shows the effectiveness of binding of CO_2 to the TiO_2 surface and the importance of the interaction of $CO_2^{-\bullet}$ with surface-bound OH groups in inducing multistep reduction process.

In summary, the electrochemical reduction of CO_2 at nanostructured TiO_2 film proceeds via a one-electron reduction as primary step. The electrocatalytic activity of TiO_2 films arises from the conversion of Ti^{4+} sites to Ti^{3+} sites at potentials more negative than −0.95 V versus NHE. Binding of CO_2 to Ti^{3+} sites assists in decreasing the potential necessary for the reduction. The electrochemical studies presented here provide the thermodynamic basis for the photocatalytic activity of TiO_2 for CO_2 reduction. However, the requirement of a more negative potential than the conduction band energy (−0.5 V vs NHE) for the electrochemical reduction of CO_2 does question the viability of TiO_2 as an effective photocatalyst for the conversion of CO_2 to methanol. Efforts are underway to carryout electrochemically assisted photocatalytic reduction of CO_2 and understand the factors controlling the formation of C_1 products.

EXPERIMENTAL SECTION

Materials. Titanium isopropoxide (Acros Organics, 98+%), tetraethylammonium perchlorate (TEAP) (Alfa Aeser, 98%), acetonitrile (AcN) (Fisher, 99.9%), ethanol (Koptec, 200 proof), alumina powder (Baikalox), and TiO_2 paste (Solaronix, Ti-Nanoxide T/SP, particle size ∼20 nm) were used without further purification. The glassy carbon electrode (GCE) (5 mm diameter) was obtained from Pine Research Instrumentation. Nafion 115 membrane was obtained from FuelCellsEtc. High purity N_2 and CO_2 gases were from Airgas and Mittler Supply Inc., respectively.

Pretreatment of Nafion Membrane. A Nafion membrane was used to separate the anodic and cathodic compartments of the electrochemical cell. Before use, the Nafion 115 membrane was pretreated to remove organic impurities using the procedure reported by Kannan et al.[44] The membrane was first boiled in 3% (v/v) H_2O_2 for 1 h, followed by boiling in distilled water for 1 h. Then the membrane was boiled in 0.5 M H_2SO_4 for 1 h, once again followed by boiling in distilled water for 1 h. This pretreated membrane was stored in distilled water.

Working Electrode Preparation. The GCE modified with TiO_2 was used as the working electrode for voltammetric experiments. The GCE was polished with alumina slurry for 2 min and washed with water, followed by ethanol. Ten microliters of 1% (v/v) titanium isopropoxide in ethanol was drop coated on the GCE and air-dried for 30 min. Toray carbon modified with TiO_2 was used as the working electrode for the electrolysis experiments. One milliliter of 1% (v/v) titanium isopropoxide in ethanol was drop coated on a 2 × 1 cm^2 area of Toray carbon. Constant air flow on top of the electrode assisted in evaporation of the solvent.

Nanocrystalline TiO_2 Electrode Preparation. A TiO_2 modified fluorine-doped tin oxide (FTO) glass plate was used as the working electrode for in situ spectroelectrochemistry experiments. FTO plates (Pilkington Glass, TEC 7, 2 mm thickness) were cleaned in detergent solution by sonication for 30 min, followed by sonication in ethanol for 10 min. A thin film of TiO_2 paste was deposited on the FTO glass plates using the doctor blade technique. The film was dried at room temperature and then at 80 °C for 1 h. TiO_2 films were further annealed at 500 °C for 1 h in air.

Electrochemical and Spectroelectrochemical Measurements. All electrochemical measurements were carried out using a *Wave Now* USB potentiostat from Pine Research Instrumentation. GCE or TiO_2 modified GCE, platinum, and Ag/Ag^+ (Ag wire in contact with 0.01 M $AgNO_3$ and 0.1 M TEAP/acetonitrile) electrodes were used as working, counter, and reference electrode, respectively. (Note that we have considered 0.55 V NHE as the potential of Ag/Ag^+ reference electrode.[45]) TEAP (0.1 M) in ACN was used as the electrolyte in all electrochemical measurements. Voltammetric experiments were performed in gastight two-compartment electrochemical cells, separated by a piece of Nafion 115 cation exchange membrane. Before electrolysis, the cathodic compartment was purged with N_2 or CO_2 gas for 30 min. Bulk electrolysis experiments for product analysis were carried out using TiO_2 modified Toray carbon paper as the working electrode.

In situ spectroelectrochemical measurements were carried out in a Varian Cary 50 Bio spectrophotometer using a three-arm spectroelectrochemical cell, under applied electrochemical potential. TiO_2 modified FTO electrode was used as working electrode with $Ag/AgNO_3$ as the reference electrode and Pt as the counter electrode.

Gas Chromatography. Electrochemical CO_2 reduction products were analyzed using a Thermo Scientific gas chromatograph equipped with a mass spectrometer. A molecular sieve 5A column was used with helium as the carrier gas at a constant pressure of 3 psi. The temperature of the oven was set at 40 °C for 5 min, followed by ramping to 100 °C at a rate of 30 °C/min for 2 min. The peak areas of the samples were compared with standard samples to determine the concentration.

ASSOCIATED CONTENT

Supporting Information

Results of cyclic voltammograms recorded after Li^+ intercalation on a TiO_2 modified GCE, methanol crossover, and the effect of water on the methanol production are presented. This

dx.doi.org/10.1021/cs500730w | ACS Catal. 2014, 4, 3249−3254

material is available free of charge via the Internet at http://pubs.acs.org.

AUTHOR INFORMATION

Corresponding Authors

*E-mail: pkamat@nd.edu.
*E-mail: jfb@nd.edu.

Notes

The authors declare no competing financial interest.

ACKNOWLEDGMENTS

The research described here was supported by a grant from the Notre Dame Sustainable Energy Initiative. The grant is NDRL No. 5011 from the Notre Dame Radiation Laboratory, which is supported by the by the Division of Chemical Sciences, Geosciences, and Biosciences, Office of Basic Energy Sciences of the U.S. Department of Energy through award DE-FC02-04ER15533. We thank Dr. Ian Lightcap for his assistance with the GC-MS measurements.

REFERENCES

(1) Windle, C. D.; Perutz, R. N. *Coord. Chem. Rev.* **2012**, *256*, 2562−2570.
(2) Costentin, C.; Robert, M.; Saveant, J. M. *Chem. Soc. Rev.* **2013**, *42*, 2423−2436.
(3) Bocarsly, A. B.; Gibson, Q. D.; Morris, A. J.; L'Esperance, R. P.; Detweiler, Z. M.; Lakkaraju, P. S.; Zeitler, E. L.; Shaw, T. W. *ACS Catal.* **2012**, *2*, 1684−1692.
(4) Barton Cole, E.; Lakkaraju, P. S.; Rampulla, D. M.; Morris, A. J.; Abelev, E.; Bocarsly, A. B. *J. Am. Chem. Soc.* **2010**, *132*, 11539−11551.
(5) Morris, A. J.; Meyer, G. J.; Fujita, E. *Acc. Chem. Res.* **2009**, *42*, 1983−1994.
(6) Whipple, D. T.; Kenis, P. J. A. *J. Phys. Chem. Lett.* **2010**, *1*, 3451−3458.
(7) Grills, D. C.; Fujita, E. *J. Phys. Chem. Lett.* **2010**, 2709−2718.
(8) Peterson, A. A.; Norskov, J. K. *J. Phys. Chem. Lett.* **2012**, *3*, 251−258.
(9) Schneider, J.; Jia, H. F.; Muckerman, J. T.; Fujita, E. *Chem. Soc. Rev.* **2012**, *41*, 2036−2051.
(10) Kamat, P. V. *J. Photochem.* **1985**, *28*, 513−524.
(11) Schrauben, J. N.; Hayoun, R.; Valdez, C. N.; Braten, M.; Fridley, L.; Mayer, J. M. *Science* **2012**, *336*, 1298−1301.
(12) Koppenol, W. H.; Rush, J. D. *J. Phys. Chem.* **1987**, *91*, 4429−4430.
(13) Chen, Y. H.; Li, C. W.; Kanan, M. W. *J. Am. Chem. Soc.* **2012**, *134*, 19969−19972.
(14) Nie, X. W.; Esopi, M. R.; Janik, M. J.; Asthagiri, A. *Angew. Chem., Int. Ed.* **2013**, *52*, 2459−2462.
(15) de Tacconi, N. R.; Chanmanee, W.; Dennis, B. H.; MacDonnell, F. M.; Boston, D. J.; Rajeshwar, K. *Electrochem. Solid-State Lett.* **2012**, *15*, B5−B8.
(16) Natesakhawat, S.; Lekse, J. W.; Baltrus, J. P.; Ohodnicki, P. R.; Howard, B. H.; Deng, X.; Matranga, C. *ACS Catal.* **2012**, *2*, 1667−1676.
(17) Costentin, C.; Drouet, S.; Robert, M.; Saveant, J. M. *Science* **2012**, *338*, 90−94.
(18) Angamuthu, R.; Byers, P.; Lutz, M.; Spek, A. L.; Bouwman, E. *Science* **2010**, *327*, 313−315.
(19) Habisreutinger, S. N.; Schmidt-Mende, L.; Stolarczyk, J. K. *Angew. Chem., Int. Ed.* **2013**, *52*, 7372−7408.
(20) Inoue, T.; Fujishima, A.; Konishi, S.; Honda, K. *Nature (London)* **1979**, *277*, 637−638.
(21) Slamet; Nasution, H. W.; Purnama, E.; Kosela, S.; Gunlazuardi, J. *Catal. Commun.* **2005**, *6*, 313−319.
(22) Varghese, O. K.; Paulose, M.; LaTempa, T. J.; Grimes, C. A. *Nano Lett.* **2009**, *9*, 731−737.
(23) Yui, T.; Kan, A.; Saitoh, C.; Koike, K.; Ibusuki, T.; Ishitani, O. *ACS Appl. Mater. Interfaces* **2011**, *3*, 2594−2600.
(24) Lee, D.; Kanai, Y. *J. Am. Chem. Soc.* **2012**, *134*, 20266−20269.
(25) Liu, L. J.; Zhao, H. L.; Andino, J. M.; Li, Y. *ACS Catal.* **2012**, *2*, 1817−1828.
(26) Yang, C.-C.; Yu, Y.-H.; van der Linden, B.; Wu, J. C. S.; Mul, G. *J. Am. Chem. Soc.* **2010**, *132*, 8398−8406.
(27) Kamat, P. V. *J. Phys. Chem. Lett.* **2012**, *3*, 663−672.
(28) Takai, A.; Kamat, P. V. *ACS Nano* **2011**, *4*, 7369−7376.
(29) Anpo, M.; Yamashita, H.; Ichihashi, Y.; Ehara, S. *J. Electroanal. Chem.* **1995**, *396*, 21−26.
(30) Ulagappan, N.; Frei, H. *J. Phys. Chem. A* **2000**, *104*, 7834−7839.
(31) Dimitrijevic, N. M.; Vijayan, B. K.; Poluektov, O. G.; Rajh, T.; Gray, K. A.; He, H.; Zapol, P. *J. Am. Chem. Soc.* **2011**, *133*, 3964−3971.
(32) Bhattacharyya, K.; Danon, A.; Vijayan, B. K.; Gray, K. A.; Stair, P. C.; Weitz, E. *J. Phys. Chem. C* **2013**, *117*, 12661−12678.
(33) He, H.; Zapol, P.; Curtiss, L. A. *J. Phys. Chem. C* **2010**, *114*, 21474−21481.
(34) Rodriguez, M. M.; Peng, X. H.; Liu, L. J.; Li, Y.; Andino, J. M. *J. Phys. Chem. C* **2012**, *116*, 19755−19764.
(35) Carlson, T.; Griffin, G. L. *J. Phys. Chem.* **1986**, *90*, 5896−5900.
(36) Hykaway, N.; Sears, W. M.; Morisaki, H.; Morrison, S. R. *J. Phys. Chem.* **1986**, *90*, 6663−6667.
(37) Seger, B.; Kamat, P. V. *J. Phys. Chem. C* **2009**, *113*, 18946−18952.
(38) (a) Frank, S. N.; Bard, A. J. *J. Am. Chem. Soc.* **1975**, *97*, 7427−7433. (b) Meekins, B. H.; Kamat, P. V. *ACS Nano* **2009**, *3*, 3437−3446.
(39) Lamy, E.; Nadjo, L.; Saveant, J. M. *J. Electroanal. Chem.* **1977**, *78*, 403−407.
(40) Hori, Y.; Wakebe, H.; Tsukamoto, T.; Koga, O. *Electrochim. Acta* **1994**, *39*, 1833−1839.
(41) Sun, L.; Ramesha, G. K.; Kamat, P. V.; Brennecke, J. F. *Langmuir* **2014**, *30*, 6302−6308.
(42) Grills, D. C.; Matsubara, Y.; Kuwahara, Y.; Golisz, S. R.; Kurtz, D. A.; Mello, B. A. *J. Phys. Chem. Lett.* **2014**, *5*, 2033−2038.
(43) Anpo, M.; Yamashita, H.; Ichihashi, Y.; Fujii, Y.; Honda, M. *J. Phys. Chem. B* **1997**, *101*, 2632−2636.
(44) Kannan, R.; Kakade, B. A.; Pillai, V. K. *Angew. Chem., Int. Ed.* **2008**, *47*, 2653−2656.
(45) Pavlishchuk, V. V.; Addison, A. W. *Inorg. Chim. Acta* **2000**, *298*, 97−102.